

# CART neurons in the lateral hypothalamus communicate with the nucleus accumbens shell via glutamatergic neurons in paraventricular thalamic nucleus to modulate reward behavior

Amit G. Choudhary<sup>1</sup> · Amita R. Somalwar<sup>1</sup> · Sneha Sagarkar<sup>2</sup> · Abhishek Rale<sup>3</sup> · Amul Sakharkar<sup>2</sup> · Nishikant K. Subhedar<sup>3</sup> · Dadasaheb M. Kokare<sup>1</sup>

Received: 25 April 2017 / Accepted: 19 October 2017 / Published online: 7 November 2017  
© Springer-Verlag GmbH Germany 2017

**Abstract** Paraventricular thalamic nucleus (PVT) serves as a transit node processing food and drug-associated reward information, but its afferents and efferents have not been fully defined. We test the hypothesis that the CART neurons in the lateral hypothalamus (LH) project to the PVT neurons, which in turn communicate via the glutamatergic fibers with the nucleus accumbens shell (AcbSh), the canonical site for reward. Rats conditioned to self-stimulate via an electrode in the right LH–medial forebrain bundle were used. Intra-PVT administration of CART (55–102) dose-dependently (10–50 ng/rat) lowered intracranial self-stimulation (ICSS) threshold and increased lever press activity, suggesting reward-promoting action of the peptide. However, treatment with CART antibody (intra-PVT) or MK-801 (NMDA antagonist, intra-AcbSh) produced opposite effects. A combination of sub-effective dose of MK-801 (0.01 µg/rat, intra-AcbSh) and effective dose of CART (25 ng/rat, intra-PVT) attenuated CART's rewarding action. Further, we screened the LH–PVT–AcbSh circuit for neuroadaptive changes induced by

conditioning experience. A more than twofold increase was noticed in the CART mRNA expression in the LH on the side ipsilateral to the implanted electrode for ICSS. In addition, the PVT of conditioned rats showed a distinct increase in the (a) c-Fos expressing cells and CART fiber terminals, and (b) CART and vesicular glutamate transporter 2 immunostained elements. Concomitantly, the AcbSh showed a striking increase in expression of NMDA receptor subunit NR1. We suggest that CART in LH–PVT and glutamate in PVT–AcbSh circuit might support food-seeking behavior under natural conditions and also store reward memory.

**Keywords** CART · Reward · Intracranial self-stimulation · Nucleus accumbens shell · Paraventricular nucleus of thalamus · Glutamate

## Introduction

The role of canonical mesolimbic dopaminergic pathway from the ventral tegmental area (VTA) to the nucleus accumbens shell (AcbSh) and prefrontal cortex (PFC) in mediating reward is well established. However, the pathway is subject to modulation by a range of inputs to the VTA and also to AcbSh. The paraventricular thalamic nucleus (PVT), located close to the midline in the dorsal thalamus, is generally known to play a role in arousal, attention and awareness (see Kirouac 2015 for review). However, recent studies have shown that this nucleus serves as a major transit point for the passage of information from the hypothalamus to striato-cortical regions and is functionally important for processing information on energy balance, arousal and food reward (Kelley et al.

Amit G. Choudhary and Amita R. Somalwar contributed equally to the work.

**Electronic supplementary material** The online version of this article (<http://doi.org/10.1007/s00429-017-1544-6>) contains supplementary material, which is available to authorized users.

✉ Dadasaheb M. Kokare  
kokaredada@yahoo.com

<sup>1</sup> Department of Pharmaceutical Sciences, Rashtrasant Tukadoji Maharaj Nagpur University, Nagpur 440 033, India

<sup>2</sup> Department of Biotechnology, Savitribai Phule Pune University, Pune 411 007, India

<sup>3</sup> Indian Institute of Science Education and Research (IISER), Dr. Homi Bhabha Road, Pune 411 008, India

2005; Dayas et al. 2008; James and Dayas 2013; Matzeu et al. 2014; Yeoh et al. 2014; Kirouac 2015).

PVT receives a strong contingent of neuronal efferents from the lateral hypothalamus (LH; Van der Werf et al. 2002; Thompson and Swanson 2003) and relays information to Acb and medial prefrontal cortex (mPFC; Moga et al. 1995; Li and Kirouac 2008; Vertes and Hoover 2008). The glutamatergic efferents from the PVT are known to terminate on the dopamine (DA) fibers in the AcbSh (Pinto et al. 2003). The electrical stimulation of the PVT triggers glutamate release from PVT terminals, which in turn acts on *N*-methyl-*D*-aspartate (NMDA) receptors in the Acb and induces DA release (Jones et al. 1989; Parsons et al. 2007). The drugs of abuse are known to influence reward behavior via their action on the NMDA receptor-dependent DA signaling in AcbSh (Sikora et al. 2016).

PVT also serves as a target for psychostimulant drugs. Acute administration of amphetamine and cocaine dose-dependently activated *c*-Fos expression in the PVT (Deutch et al. 1998). Moreover, lesioning or silencing of PVT prevented the expected responses to ethanol and cocaine (Young and Deutch 1998; Hamlin et al. 2009; James et al. 2010).

A good deal of information is available on the LH–PVT segment of the circuit. The LH–medial forebrain bundle (MFB) area shows a rich assemblage of orexin, neuropeptide Y (NPY) or melanocyte-concentrating hormone (MCH) containing neurons projecting into the PVT (Lee et al. 2015). These neuropeptides convey feeding, arousal, anxiety and reward-related information across the LH–PVT–Acb axis and modulate psychostimulant-triggered actions (Kelley et al. 2005; Dayas et al. 2008; Li et al. 2010a, b; Choi et al. 2012; Matzeu et al. 2015, 2016). Several studies underscore the relevance of PVT in processing reward-related information following pharmacological manipulations (Choi et al. 2012; Matzeu et al. 2015, 2016; Neumann et al. 2016). CART is yet another neuropeptide abundantly expressed in the LH–MFB neurons (Koyle et al. 1997) and several of these are known to contain GABA (Elias et al. 2001). In recent years, the role of CART in modulating drug-induced reward has been recognized (Kuhar et al. 2005; Philpot and Smith 2006; Rademacher et al. 2010; Upadhyaya et al. 2012). Intracerebroventricular (Icv) or intra-VTA microinjection of CART increased the concentration of DA and its metabolites in the Acb (Yang et al. 2004; Kuhar et al. 2005) and induced conditioned place preference (CPP) in rats (Kimmel et al. 2000). Activation of hypothalamic CART neurons has been implicated in the conditioned reinstatement of ethanol relapse (Dayas et al. 2008). Intra-PVT injections of CART attenuated cocaine self-infusion behavior by negatively modulating PVT (James et al. 2010). Application of CART significantly attenuated cocaine-triggered excitability of

PVT neurons (Yeoh et al. 2014). Studies from our laboratory showed that CART neurons in the LH area modulate reward associated with binge eating in rats (Bharne et al. 2015).

In a recent study, we have shown that CART neurons in the LH–MFB area project into the posterior VTA (pVTA) and play an important role in mediating reward (Somalwar et al. 2017). In addition, there is anatomical evidence to suggest a role for CART in the LH–PVT circuit. The CART neurons in the LH–MFB region project into the PVT (Kirouac et al. 2006; Parsons et al. 2006), make synaptic contacts with the target neurons and send divergent axonal collaterals to the AcbSh (Lee et al. 2015). In spite of the above, the role of CART in modulating reward in the LH–PVT–AcbSh circuit has not been examined in behaving animals. In this study, we test the hypothesis that CART neurons in the LH communicate with the glutamatergic neurons of the PVT, which in turn transmit the information to AcbSh and influence reward and reinforcement behavior.

Traditionally, studies aimed at investigating reward mechanisms have employed drug administration protocols. However, drugs may exercise non-specific pharmacological effects which tend to confound interpretation. On the contrary, intracranial self-stimulation (ICSS) serves as a surrogate for the natural reward, and provides a simple, reliable and quantitatively reproducible tool (Wise 1996). In the present study, the rats were implanted with bipolar electrode targeted at the LH–MFB and conditioned to press the lever in an operant chamber to gain electrical self-stimulation. We test if CART, stereotaxically targeted at PVT, can modulate the lever press activity. Since glutamatergic neurons in the PVT evoke DA release in the AcbSh (Parsons et al. 2007), there is a possibility that the glutamatergic system may mediate the rewarding action of CART. Therefore, we employed MK-801 (NMDA receptor antagonist given via the intra-AcbSh route), with and without CART (intra-PVT), and monitored the ICSS activity. The neuroadaptive changes due to ICSS experience in the operant chamber were evaluated in terms of alterations in the CART mRNA expression in the LH–MFB area. The changes in the CART fiber innervation of the PVT, coupled with activation of neurons as revealed by *c*-Fos, were evaluated using immunohistochemistry. To examine the possibility of cross talk between CART fiber terminals and glutamatergic neurons in the PVT region, CART and vesicular glutamate transporter 2 (vGLUT2; a marker for glutamatergic neurons; Herzog et al. 2001; Huang et al. 2006) proteins were immunolabeled in the PVT of unconditioned (control) and conditioned rats. Further, we tested the effect of ICSS conditioning on NMDA receptor expression in the AcbSh using antibodies against its subunit NR1 (NMDAR1) in the immunohistochemistry protocol.

## Materials and methods

### Experimental animals

Adult male Wistar rats weighing 220–260 g were group housed in polypropylene cages and maintained at  $25 \pm 2$  °C and 12:12 h light/dark cycle, light on at 0700 h. The rats had free access to food (Trimurti Feeds, Nagpur, India) and water. The behavioral assessment was conducted during the light cycle between 0900 and 1400 hours. All experimental protocols were employed under strict compliance with the Institutional Animal Ethics Committee (IAEC), Department of Pharmaceutical Sciences, Rashtrasant Tukadoji Maharaj Nagpur University, Nagpur, India.

### Surgery for intra-AcbSh, intra-PVT cannulation, intra-LH-MFB electrode implantation and habituation of rats

The procedure of stereotaxic surgery has been standardized in our laboratory (Dandekar et al. 2008; Nakhate et al. 2009). Rats were anesthetized with thiopentone sodium (50 mg/kg; intraperitoneal, ip, Neon Laboratories Ltd, Mumbai). The hair was removed by applying the hair depilator (Anne French Cream, Wyeth Limited, Mumbai, India) on the head and then rats were placed in a stereotaxic instrument (David Kopf Instruments, USA). Following a mid-sagittal incision on the scalp, the bregma was located. A set of rats was implanted with a bipolar electrode, prepared in-house (Desai et al. 2014), in the right LH-MFB (AP – 2.8 mm, ML – 1.7 mm, DV – 8.5 mm) and with a 24-gauge stainless steel guide cannula (Kokare et al. 2011) unilaterally in the right PVT (AP – 1.8 mm, ML – 0.8 mm, DV – 5.1 mm ventral from the surface of the skull at 10° angle to the vertical) for delivery of artificial cerebrospinal fluid (aCSF), non-immune serum (NIS), CART or CART antibody (CART-Ab). Another group of animals was implanted with bipolar stimulating electrode in the right LH-MFB (co-ordinates given above) and with guide cannula in the right AcbSh (AP +0.7 mm, ML – 0.8 mm, DV – 6.5 mm) for MK-801 administration. Additional groups of animals were implanted with bipolar electrode in the right LH-MFB, cannulae in the right PVT and AcbSh (Paxinos and Watson 1998) and used for combination treatment with MK-801 (intra-AcbSh) and CART peptide (intra-PVT). Guide cannula and electrode were secured to the skull and a flush-fitting stylet was inserted into the guide cannula to prevent blockage (Kokare et al. 2011). Following surgery, the animals were allowed to recover for 7 days. During this period, from day 4 onward, the rats were habituated to gentle handling for

about 5 min each day. The rats were then divided into separate groups with five to six animals in each and conditioned in the operant chamber for electrical self-stimulation.

The position of the electrodes and guide cannulae was confirmed in post-necropsy brain sections. In the ICSS experiment, out of a total of 85 rats, 61 were found with correct placement of electrode and guide cannulae (Supplementary Figs. 1–3). The rats in which the cannulae or electrodes missed the target could not be trained. The data from the animals with correct placement of electrode or guide cannulae were considered for the statistical analyses.

### Procedure for operant conditioning

The rats were allowed to self-stimulate via an electrode implanted into the LH-MFB. The conditioning apparatus (Coulbourn Instruments, USA) consists of a sound-attenuating acrylic test chamber (30.48 × 25.40 × 30.48 cm) equipped with the grid floor and active and inactive levers located 3 cm above the floor. The simulation light positioned 8 cm above the active lever was illuminated after each lever pressing. The operant chamber was equipped with continuous glowing 2-W white house light, which was placed on the opposite wall of the lever and a fan was switched on throughout the experiment for white noise. In addition, a stimulator (Coulbourn Instruments, USA) was placed with the test chamber and the electrode was connected to the stimulator via a swivel connector. The stimulator was controlled by a computer software program that controlled all the programming parameters and data collection (Graphic State® 3.0).

With reference to conditioning of animals, we followed the procedure described by Somalwar et al. (2017) which has been standardized in our laboratory. One week after surgery, rats were trained in the operant chamber on a continuous reinforcement schedule (FR1) to press the lever for electrical self-stimulation. Each active lever press by the animal illuminated the cue light and delivered a 0.5 s train of square-wave cathodal pulses (0.1 ms pulse duration) at a definite frequency of 186 Hz [ $\log(2.270)$ ]. The frequency was varied instead of intensity of stimulation, since such manipulations activated the same population of neurons. The stimulation current (100–300  $\mu$ A) was gradually adjusted for each rat. During ICSS conditioning, the cathodal current was used. The use of the cathodal current is appropriate, not only because it allows conditioning at lower stimulation parameters, but also because prolonged application of anodal current may lesion the tissue (Carlezon and Chartoff 2007; Somalwar et al. 2017). During the acquisition phase, the animals were trained to self-

stimulate for at least three consecutive days, using stimulation parameters that maintain near maximal rates of response/lever press activity. After acquisition of the behavior, each rat was subjected to 15 trials of descending series of frequencies (often called as a ‘pass’) of 1 min each. One minute frequency trial comprised 5 s priming phase, 50 s test phase and 5 s time-out phase, where each 1 s phase delivered electrical pulses for 500 ms, followed by 500 ms time-out (no stimulation). During the initial 5 s priming phase, non-contingent stimulations were delivered. Following the primes, there was a 50 s test phase in which the number of lever pressings was recorded. During the last 5 s interval period, no stimulation was delivered and this completed the 1 min frequency trial. The stimulation frequency was then reduced by about 10% (0.05 log<sub>10</sub> units) and another trial (pass) was initiated. Reward and reinforcement were evaluated in terms of the lever press activity and represented as rate–frequency curves and ICSS threshold ( $M_{50}$  and  $T_0$ ) (Negus and Miller 2014; Somalwar et al. 2017). The frequency that maintains 50% of maximal response is often called ‘half maximum’ or  $M_{50}$  value. The frequency at which the stimulation becomes rewarding and where the line intersects the  $x$ -axis is considered as ‘Theta-0’ ( $T_0$ ; rate of responding > 0). The ICSS threshold ( $M_{50}$  and  $T_0$ ) was calculated using nonlinear regression curve fit method using GraphPad Prism 5 software (Coulombe and Miliareisis 1987; Somalwar et al. 2017). The leftward shift in the rate–frequency curve function indicated reward facilitation, while the rightward shift suggested reward attenuation (Wise 1996; Negus and Miller 2014). Once the ICSS threshold was stabilized (< 10% variation), the dose-dependent effects of CART, CART-Ab and MK-801 in the behavioral test were evaluated. With a view to test the involvement of NMDA receptors in CART-mediated activation of the mesolimbic reward system, MK-801 and CART were co-administered. On each test day, three passes were obtained for each animal prior to the drug treatment. In each drug-treated animal, three to four additional rate–frequency curves were generated.

### Drug solutions and administrations

CART (55–102; Phoenix, cat. no. 003-62) and monoclonal CART-Ab (generous gift from Drs. Lars Thim and Jes Clausen) were dissolved in 0.2 M phosphate buffer and diluted to a final concentration in artificial cerebrospinal fluid (aCSF), while MK-801 (Sigma-Aldrich, St. Louis, MO, USA, cat. no. M107) was dissolved in double distilled water. These agents were stored at  $-20^{\circ}\text{C}$  as stock solutions. The final dilutions were made with aCSF and injected stereotaxically using a microliter syringe (Hamilton, NV, USA).

A dose-dependent study of CART and MK-801 was carried out in operant conditioned animals ( $n = 5\text{--}6$  per group). Rats were administered aCSF (0.25  $\mu\text{l}/\text{rat}$ , intra-PVT or AcbSh), NIS (0.25  $\mu\text{l}/\text{rat}$ , intra-PVT), CART (10–50 ng/0.25  $\mu\text{l}/\text{rat}$ , intra-PVT), CART-Ab (1:500, 0.25  $\mu\text{l}/\text{rat}$ ; intra-PVT) and MK-801 (0.01–0.1  $\mu\text{g}/0.25 \mu\text{l}/\text{rat}$ , intra-AcbSh). Fifteen minutes post-intra-nuclear infusions, the effects on reward behavior were evaluated in an operant chamber.

With a view to finding out the modulatory effect of MK-801 on the rewarding effect of CART, separate groups of animals ( $n = 5\text{--}6$  per group) were subjected to the following treatments: (1) aCSF + aCSF, (2) aCSF + CART, (3) aCSF + MK-801 and (4) MK-801 + CART. The relevant details are furnished below: aCSF (0.25  $\mu\text{l}/\text{rat}$ , intra-PVT) or MK-801 (0.01  $\mu\text{g}/0.25 \mu\text{l}/\text{rat}$ , intra-AcbSh) injected 15 min prior to CART (25 ng/0.25  $\mu\text{l}/\text{rat}$ , intra-PVT). Fifteen minutes thereafter, the rats were subjected to ICSS test in the operant chamber. Following the ICSS test, the individual animal was evaluated for locomotor activity in an open field arena and the number of crossovers was measured.

### Assessment of locomotor activity

To test the possible involvement of locomotor component in the reward behavior following various treatments, an open field test (OFT) was employed (Dandekar et al. 2008). Immediately after the operant task, the rat was individually placed at the center of the OFT apparatus, and the number of crossovers were monitored over a period of 10 min.

The effect of different treatments with aCSF (0.25  $\mu\text{l}/\text{rat}$ , intra-PVT), CART (10–50 ng/rat, intra-PVT), NIS (0.25  $\mu\text{l}/\text{rat}$ , intra-PVT), CART-Ab (1:500 dilution, intra-PVT) and MK-801 (0.01–0.1  $\mu\text{g}/\text{rat}$ , intra-AcbSh) on locomotor activity has been summarized in Table 1. No statistically significant differences were found across the treatment and control groups ( $p > 0.05$ ).

### Immunohistochemistry

Brains from the control and operant conditioned rats were isolated, cryoprotected (25% sucrose), embedded and serially sectioned on a cryostat (Leica CM-1850, Leica Microsystems, Germany) at 30  $\mu\text{m}$  thickness in the coronal plane. The sections passing through PVT were processed for double immunolabeling with antibodies in the following combinations: (a) anti-mouse CART (1:5000) and anti-rabbit c-Fos (1:500; Santa Cruz Biotechnology; cat. no. sc-52); (b) anti-mouse CART and anti-rabbit vGLUT2 (1:4000; Abcam; cat. no. ab181773). Additionally, the brain sections passing through the AcbSh were incubated for single immunolabeling with antibodies against NR1 (polyclonal rabbit NMDAR1, dilution 1:500; Cell

**Table 1** Effect of operant conditioning and various treatments on locomotor activity

Sr. no.	Groups	Treatments	Dose	Number of crossovers $\pm$ SEM
1	Unconditioned	aCSF	0.25 $\mu$ l/rat	66.67 $\pm$ 3.11
2	Operant conditioned	aCSF	0.25 $\mu$ l/rat	68.83 $\pm$ 3.68
		CART	10 ng/rat	64.28 $\pm$ 3.63
			25 ng/rat	66.57 $\pm$ 4.42
			50 ng/rat	69.00 $\pm$ 4.82
		NIS	0.25 $\mu$ l/rat	65.67 $\pm$ 3.26
		CART-Ab	1:500 dilution	61.83 $\pm$ 2.72
		MK-801	0.01 $\mu$ g/rat	63.17 $\pm$ 2.77
			0.05 $\mu$ g/rat	58.50 $\pm$ 2.52
		0.1 $\mu$ g/rat	60.50 $\pm$ 2.34	

signaling; cat. no. 5704). All the sections were incubated overnight at 4 °C, washed in PBS and incubated either in a single or cocktail of respective secondary antibodies using Alexa Fluor-488 conjugated anti-mouse IgG or Alexa Fluor-568 conjugated anti-rabbit IgG (Jackson Immuno Research; 1:500 each) for 2 h at room temperature. Finally, sections were washed, mounted (medium: 50% glycerol, 0.5% *N*-propyl-gallate, 20 mM Tris, pH 8.0) containing 4',6-diamidino-2-phenylindole (DAPI; 1  $\mu$ g/ml) and observed under Leica DM-2500 (Leica Microsystems, Germany) fluorescence microscope using suitable dual filter sets, and the images were captured. The representative images were taken on a laser scanning confocal microscope (Zeiss LSM 710, Carl Zeiss, Germany) and merged using ImageJ 1.45 software. To test the specificity of the immunoreaction, the following steps were carried out. The specificity of CART antibody was tested in an earlier study from our laboratory (Dandekar et al. 2008, 2009). Briefly, application of 1 ml diluted antibody, pre-incubated with CART (55–102) at  $10^{-5}$  M for 24 h, completely failed to produce immunoreaction. The primary antibody against vGLUT2, c-Fos or NR1 was omitted and replaced with bovine serum albumin (BSA); these sections did not produce immunoreaction.

### Morphometric analyses

The immunostained sections were subjected to relative quantitative analyses according to the procedure described earlier (Somalwar et al. 2017). The percentage (%) immunoreactive area occupied by CART fibers (green) and the number of c-Fos cells (red) were evaluated in the PVT of unconditioned and conditioned rats using microscopic images from predetermined areas in the sections. Similarly, the percentage (%) immunoreactive areas occupied by CART fibers (green) and vGLUT2 elements (red) were evaluated from the double-labeled sections through the PVT. The percentage (%) immunoreactive area occupied by NR1 subunit elements in the AcbSh was evaluated across the different groups.

The images of brain section were digitized, the background was considered as threshold, and percent area occupied by immunostained elements was measured based on individual pixel intensity in all the control and ICSS-conditioned groups using ImageJ software (National Institutes of Health, Bethesda, MD, USA). Five sections passing through the PVT or AcbSh of each brain were processed for single or double immunolabeling. Ten measurements of both sides of the five sections were taken and the data from five brains in each group were collated ( $n = 5$  each group). The immunoreactivity in the predetermined rectangular area ( $691 \times 578 \mu\text{m}$  demarcated in Figs. 3 and 5) and square area ( $135 \times 135 \mu\text{m}$  demarcated in Fig. 4) was evaluated. The data for each nuclear group or area from all animals in each group were pooled and the mean  $\pm$  standard error of mean (SEM) was calculated. The measurements were taken by the investigator blind to the treatment.

### DiI retrograde neuronal tracing

To explore the connectivity between the AcbSh and PVT, rats ( $n = 3$ ) were unilaterally implanted with cannulae targeted at right AcbSh and the right lateral ventricle. After 7 days of recovery, animals were injected with retrograde tracer DiI [1,1'-dioctadecyl-3,3,3',3'-tetramethylindocarbocyanine perchlorate (1%; 0.25  $\mu$ l/rat, intra-AcbSh; cat. no. 42364, Sigma)] prepared in dimethyl sulfoxide. Following an interval of 13 days, the rats were injected with colchicine (60  $\mu$ g/5  $\mu$ l/rat, icv) and after 24 h perfused transcardially with PBS, followed by 4% paraformaldehyde fixative. Brains were isolated, cryoprotected and embedded, and coronal sections (30  $\mu$ m thickness) passing through the PVT were taken on a cryostat. Sections were processed for CART immunolabeling using anti-mouse CART primary antibody and later with Alexa Fluor 488-conjugated anti-rabbit IgG (dilution 1:400; Jackson ImmunoResearch, West Grove, PA, USA) secondary antibody as described in “Immunohistochemistry”.

## Quantitative real-time PCR for CART mRNA measurements

CART transcript levels were analyzed using quantitative real-time PCR (qRT-PCR) as described previously by Sakharkar et al. (2014). Immediately after the ICSS tasks, the brains of six conditioned rats were separated, quickly frozen and stored at  $-80^{\circ}\text{C}$ . Six brains of unconditioned rats were similarly processed and used as controls. The LH area from the contralateral and ipsilateral side of each brain was separated and RNA was isolated using TRIZOL reagent (Life Technologies, Grand Island, NY, USA). DNA was removed using DNA-free<sup>TM</sup> Kit (Life Technologies). Purified RNA was reverse-transcribed using High Capacity cDNA Reverse Transcription kit (Applied Biosystems, USA) and cDNA was subjected to qRT-PCR (SYBR Green qPCR Master Mix, Applied Biosystems) on CFX96 real-time PCR machine (Bio-Rad). NCBI Primer Blast tool was used to design the CART primer to measure CART transcript in the brain of rat. The primer sequences and qRT-PCR conditions used in this study are as follows: CART Rat mRNA (F-5'-GGATGATGCGTCCCATG-3'; R-5'-G'GAACCGAAGGAGGCTGTCACC-3') and  $\beta$ -actin (F-5'-TGTGATGGTGGGAATGGGTCAG-3'; R-5'-TTT GATGTCACGCACGATTTC-3').

qRT-PCR conditions: 10 min at  $95^{\circ}\text{C}$ , followed by 40 cycles at  $95^{\circ}\text{C}$  for 30 s,  $57^{\circ}\text{C}$  for 30 s, and  $72^{\circ}\text{C}$  for 30 s, then  $95^{\circ}\text{C}$  for 15 s and  $60^{\circ}\text{C}$  for 1 h. For normalization,  $\beta$ -actin was used as an internal control. Each reaction was performed in duplicate. Relative expression of CART was analyzed using the  $2^{-\Delta\Delta C_T}$  method (Livak and Schmittgen 2001). Fold changes were calculated after considering the contralateral as control for the respective ipsilateral samples and the results are represented as mean fold changes ( $\pm$  SEM) in different groups.

## Data analyses

Data obtained from the behavioral studies were separately pooled, averaged and represented as mean  $\pm$  SEM. The rate–frequency curves were represented by the curve fit method and statistically analyzed by two-way ANOVA with 95% confidence level, using GraphPad Prism 5 software. The ICSS threshold ( $M_{50}$  and  $T_0$ ) was calculated using nonlinear regression curve fit method and analyzed using one-way ANOVA, followed by post hoc Bonferroni's multiple comparison test. The immunofluorescence data were analyzed using one-way ANOVA or unpaired  $t$  test. Post hoc analyses were performed with Bonferroni's multiple comparison test. The CART mRNA levels were analyzed using one-way ANOVA, followed by post hoc comparisons using Tukey's multiple comparison test. For

all the analyses, a value of  $p < 0.05$  was considered to be significant.

## Results

### Response of the operant conditioned rat

As reported in our earlier studies (Desai et al. 2013; Somalwar et al. 2017), rats conditioned to self-stimulate via an electrode in the LH–MFB area showed an incremental lever press activity with the application of higher-frequency current and a maximum of 35–40 lever presses (per 50 s) were recorded at 165 Hz [ $\log(2.217)$ ]. However, the lever press activity was depressed at higher frequencies (186 Hz) [ $\log(2.270)$ ]. The application of lower frequencies linearly reduced the response, and the frequency that produced 50% of maximum response was considered as  $M_{50}$ . The minimum lever press activity was detected at 59–66 Hz [ $\log(1.771)$ – $\log(1.820)$ ] and this was considered Theta-0 ( $T_0$ ).

### CART (intra-PVT) dose-dependently increased the lever press activity and lowered the ICSS threshold

CART given via the PVT route (25 and 50 ng/rat) significantly increased the number of lever pressings and lowered the ICSS threshold, as indicated by a leftward shift in the rate–frequency curve [factor 'frequency'  $F_{15,400} = 533.4$ ,  $p < 0.0001$ ; factor 'treatments'  $F_{4,400} = 155.6$ ,  $p < 0.0001$  and interaction 'treatment'  $\times$  'frequency'  $F_{60,400} = 3.791$ ,  $p < 0.0001$ ]. This suggested amplification of the ICSS activity by CART (Fig. 1b). Application of one-way ANOVA showed a significant decrease in  $M_{50}$  [ $F_{4,29} = 13.05$ ,  $p < 0.0001$ ] and  $T_0$  [ $F_{4,29} = 37.12$ ,  $p < 0.0001$ ]. Post hoc Bonferroni's multiple comparison test revealed that CART at the doses of 25 and 50 ng/rat produced significant decrease in  $M_{50}$  ( $p < 0.01$  and  $p < 0.001$ , respectively) and  $T_0$  ( $p < 0.01$  and  $p < 0.001$ , respectively) compared to that following aCSF treatment (Fig. 1c, d). However, at lower dose (10 ng/rat), CART failed to influence the ICSS threshold.

### CART antibody (intra-PVT) decreased lever press activity and elevated the ICSS threshold

Application of CART antibodies (1:500 dilution, intra-PVT) significantly reduced contingent lever pressings and elevated ICSS threshold as reflected by the rightward shift in the frequency–response curve (factor 'frequency'  $F_{15,192} = 278.2$ ,  $p < 0.0001$ ; factor 'treatments'  $F_{2,192} = 208.4$ ,  $p < 0.0001$  and interaction 'treatment'  $\times$  'frequency'  $F_{30,192} = 9.774$ ,

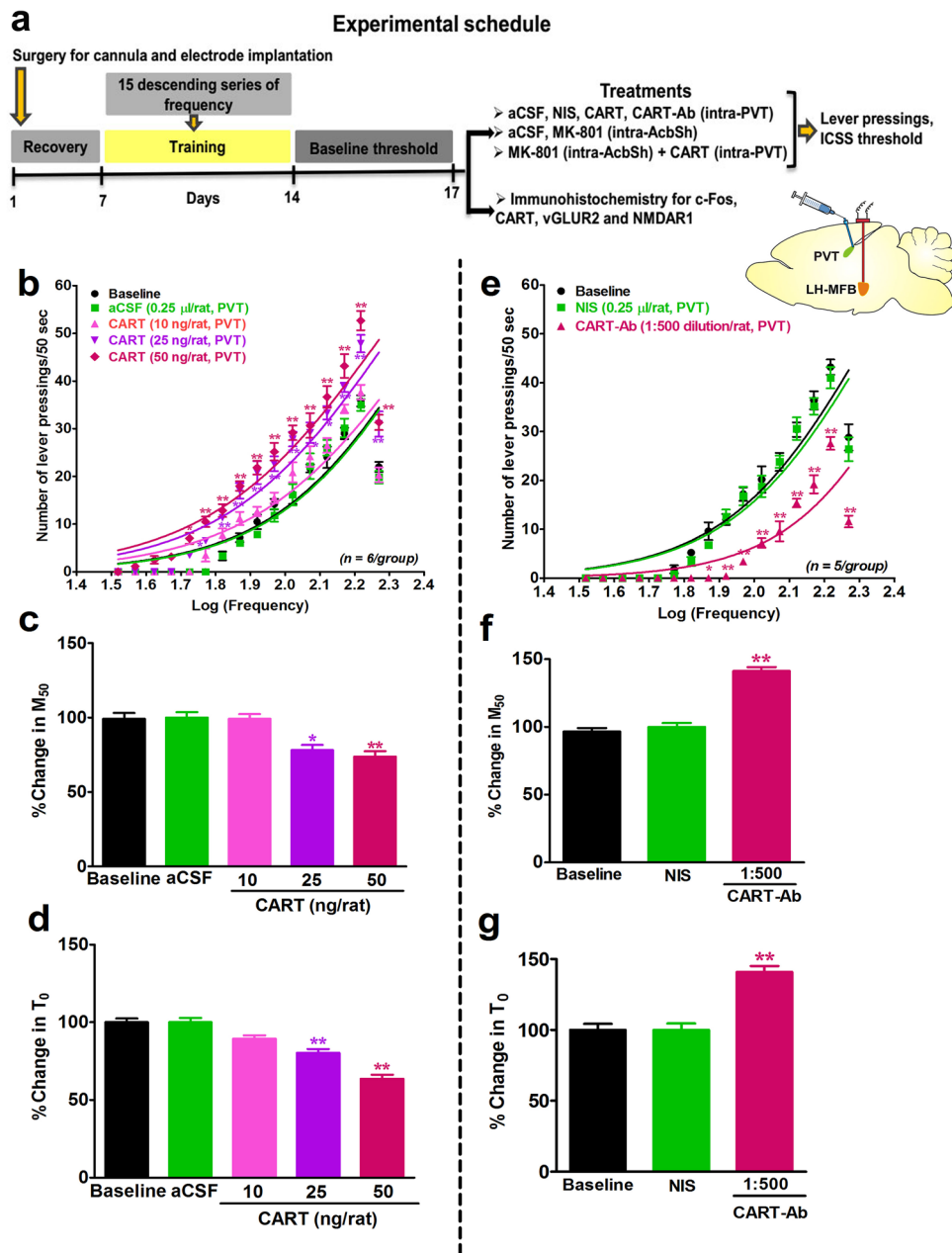


**Fig. 1** Flowchart (a) summarizes the schedule of surgery, recovery, training, treatments and behavioral assay in an operant chamber and tissue processing. The effects of various treatments [artificial cerebrospinal fluid (aCSF), non-immune serum (NIS), cocaine- and amphetamine-regulated transcript peptide (CART, 10–50 ng/rat) or CART antibody (CART-Ab, 1:500 dilution)] on lever pressings,  $M_{50}$  and  $T_0$  have been summarized (b–g). Brain schematic indicates the

position of the electrode in the lateral hypothalamus (LH)–medial forebrain bundle (MFB) and cannula in the paraventricular nucleus of thalamus (PVT). The rate–frequency curves were analyzed by nonlinear regression curve fit method, and the percentage  $M_{50}$  and  $T_0$  thresholds were analyzed using one-way ANOVA followed by post hoc Bonferroni’s multiple comparison test. \* $p < 0.01$ , \*\* $p < 0.001$  versus respective control

$p < 0.0001$ ) (Fig. 1e). Application of one-way ANOVA showed a significant increase in  $M_{50}$  ( $F_{2,14} = 76.65$ ,  $p < 0.0001$ ) and  $T_0$  ( $F_{2,14} = 29.91$ ,  $p < 0.0001$ ) following CART antibody treatment. The post hoc Bonferroni’s test revealed that CART antibody (1:500 dilution), increased  $M_{50}$  ( $p < 0.001$ ) and  $T_0$  ( $p < 0.001$ ) as compared to that in the NIS control rats (Fig. 1f, g).

position of the electrode in the lateral hypothalamus (LH)–medial forebrain bundle (MFB) and cannula in the paraventricular nucleus of thalamus (PVT). The rate–frequency curves were analyzed by nonlinear regression curve fit method, and the percentage  $M_{50}$  and  $T_0$  thresholds were analyzed using one-way ANOVA followed by post hoc Bonferroni’s multiple comparison test. \* $p < 0.01$ , \*\* $p < 0.001$  versus respective control

### MK-801 (intra-AcbSh) decreased lever press activity and elevated the ICSS threshold

Microinjections of MK-801 (0.01–0.1  $\mu\text{g}/\text{rat}$ ) in the AcbSh dose-dependently decreased the lever press activity and increased ICSS threshold, as indicated by the rightward shift in the rate–frequency curve (factor ‘frequency’

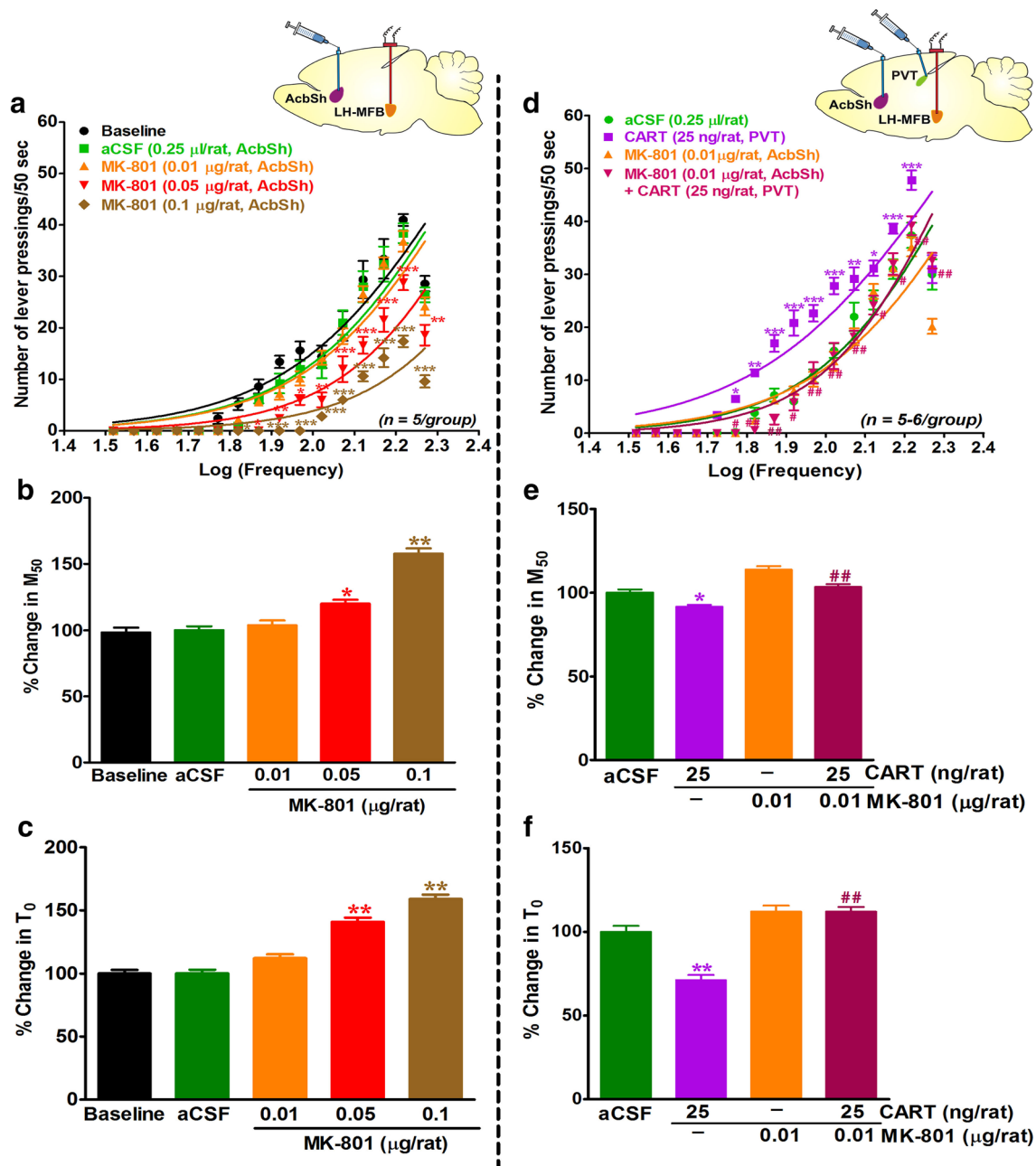


**Fig. 2** Modulation of intracranial self-stimulation (ICSS) activity by MK-801 (a–c) and MK-801 + CART (d–f). Brain schematics indicate the position of the electrode in the lateral hypothalamus (LH)–medial forebrain bundle (MFB) and cannulae in the nucleus accumbens shell (AcbSh) and paraventricular nucleus of thalamus (PVT) (a, d). Dose-dependent effect of MK-801 (0.01–0.1  $\mu\text{g}/\text{rat}$ ), administered in the AcbSh, on the number of lever pressings (a),  $M_{50}$  (b) and  $T_0$  (c), and modulation of the CART (25 ng/rat, intra-PVT)-

induced ICSS activity in rats pre-treated with MK-801 (0.01  $\mu\text{g}/\text{rat}$ , intra-AcbSh) (d–f). The rate–frequency curves were analyzed by nonlinear regression curve fit method, and the percentage  $M_{50}$  and  $T_0$  thresholds were analyzed using one-way ANOVA followed by post hoc Bonferroni’s multiple comparison test. \* $p < 0.05$ , \*\* $p < 0.01$ , \*\*\* $p < 0.001$  versus aCSF control and # $p < 0.01$ , ## $p < 0.001$  versus CART per se treated rats

$F_{15,320} = 319.7$ ,  $p < 0.0001$ ; factor ‘treatments’  $F_{4,320} = 129.0$ ,  $p < 0.0001$  and interaction ‘treatment’  $\times$  ‘frequency’  $F_{60,320} = 7.208$ ,  $p < 0.0001$ , suggesting reward attenuating effect (Fig. 2a). Based on these curves, the  $M_{50}$  and  $T_0$  were calculated for aCSF and each dose of

the MK-801. Application of one-way ANOVA showed a significant increase in  $M_{50}$  ( $F_{4,24} = 51.89$ ,  $p < 0.0001$ ) and  $T_0$  ( $F_{4,24} = 70.32$ ,  $p < 0.0001$ ) following MK-801 treatment. The post hoc Bonferroni’s test revealed that MK-801, at the doses of 0.05 and 0.1  $\mu\text{g}/\text{rat}$ , resulted in a dose-



dependent increase in  $M_{50}$  ( $p < 0.01$  and  $p < 0.001$ , respectively) and  $T_0$  ( $p < 0.01$  and  $p < 0.001$ , respectively) as compared to that in the conditioned control rats (Fig. 2b, c).

### MK-801 pre-treatment attenuated CART-induced facilitative effect on ICSS

With a view to evaluate the involvement of NMDA receptors in CART-promoted ICSS activity, a combination study was performed. A sub-effective dose of MK-801 (0.01  $\mu\text{g}/\text{rat}$ , via AcbSh) was injected prior to the effective dose of CART (25 ng/rat, intra-PVT). CART-induced increase in lever press activity was significantly attenuated in MK-801 pre-treated animals (Fig. 2d). Administration of MK-801 with CART significantly shifted the rate–frequency curve towards the right as compared to that in CART per se group (factor ‘frequency’  $F_{15,272} = 399.9$ ,  $p < 0.0001$ ; factor ‘treatments’  $F_{3,272} = 107.9$ ,  $p < 0.0001$  and interaction ‘treatment’  $\times$  ‘frequency’  $F_{45,272} = 5.239$ ,  $p < 0.0001$ ). The application of one-way ANOVA showed a significant effect of MK-801 treatment for  $M_{50}$  ( $F_{3,20} = 28.71$ ,  $p < 0.0001$ ) and  $T_0$  ( $F_{3,20} = 35.10$ ,  $p < 0.0001$ ) (Fig. 2e, f). Application of post hoc Bonferroni’s multiple comparisons test revealed that pre-treatment of MK-801, at the sub-effective dose of 0.01  $\mu\text{g}/\text{rat}$

coupled with the CART, resulted in elevation of  $M_{50}$  ( $p < 0.05$ ) and  $T_0$  ( $p < 0.001$ ) relative to CART per se treated group (Fig. 2e, f).

### Effect of conditioning on the expression of CART and c-Fos in the PVT

In the control rat, CART fibers showed rich innervation of the posterior PVT concurrent with few c-Fos-labeled cells. However, the ICSS conditioning resulted in  $\sim 2$ -fold increase in the population of CART fibers ( $p < 0.001$ ) and  $\sim 3$ -fold increase in the number of c-Fos cells in the PVT ( $p < 0.001$ ) (Fig. 3a–f). This suggested the possibility of increased CARTergic inputs to the PVT and concomitant stimulation of the target neurons.

### Effect of conditioning on the expression of CART and vGLUT2 in the PVT

The percent immunoreactivity of CART fibers and vGLUT2 elements was significantly increased in the PVT of the animals conditioned to self-stimulate versus that in the unconditioned rats ( $p < 0.001$ ; Fig. 4a–f). The CART fibers were noticed in the close vicinity of vGLUT2 immunoreactive elements (glutamatergic neurons) in the conditioned rats (Fig. 4f).

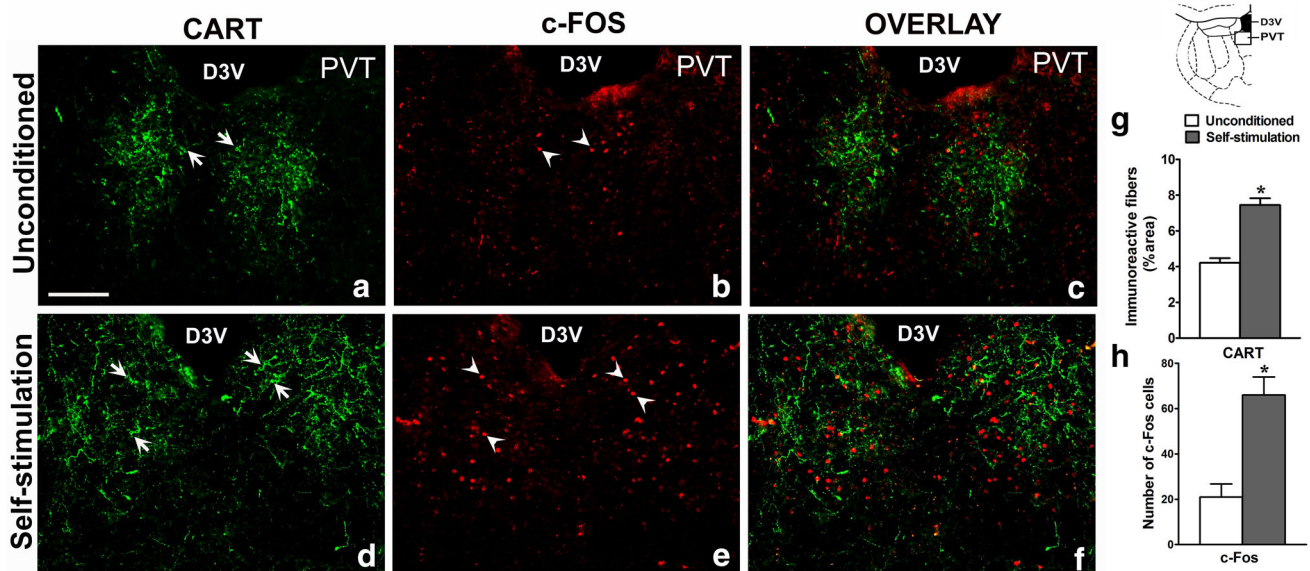


**Fig. 3** Coronal sections through the paraventricular nucleus of thalamus (PVT) showing CART immunoreactive fibers (green, arrows; **a**, **d**), c-Fos cells (red, arrowheads; **b**, **e**) and overlay (CART and c-Fos; **c**, **f**) in unconditioned (**a–c**) and conditioned (**d–f**) rats. Data on the percent (%) immunoreactive area covered by CART fibers and the number of c-Fos cells are represented in ‘g’ and ‘h’

respectively ( $n = 5$  in each group). The data were collated from the demarcated rectangular area shown in the schematic (not to scale) taken from Paxinos and Watson (1998) coordinates (AP – 1.8 mm to bregma). The data were analyzed by unpaired  $t$  test. \* $p < 0.001$  versus unconditioned rats. D3V dorsal third ventricle. Scale bar = 100  $\mu\text{m}$ . Magnification is same in ‘a–f’

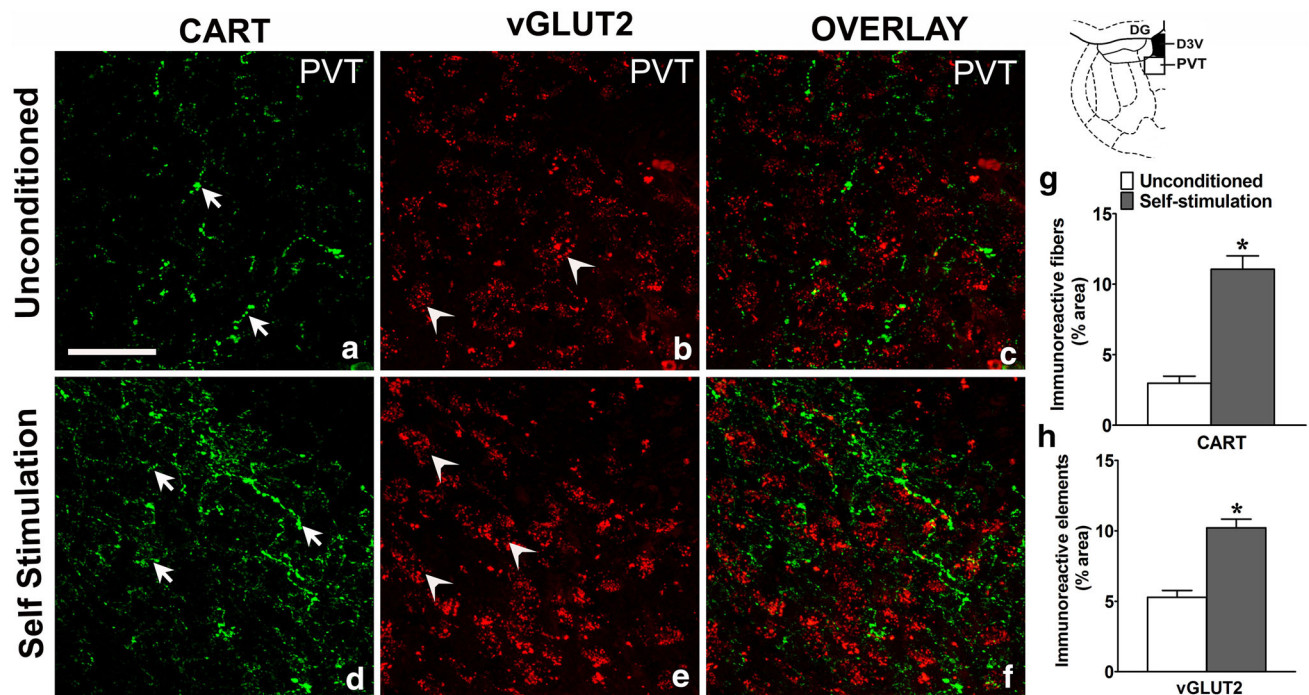


**Fig. 4** Coronal sections through the paraventricular nucleus of thalamus (PVT) showing the CART fibers (green, arrows; **a**, **d**) and vGLUT2 immunoreactive elements (red, arrowheads; **b**, **e**), and overlay (CART and vGLUT2; **c**, **f**) in unconditioned and conditioned rats. Data on the percent (%) immunoreactive area covered by CART fibers and vGLUT2 elements are represented in ‘g’ and ‘h’

respectively ( $n = 5$  in each group). The data were collated from the demarcated square area shown in the schematic (not to scale) taken from Paxinos and Watson (1998) coordinates (AP  $- 1.8$  mm to bregma). The data were analyzed by unpaired  $t$  test. \* $p < 0.001$  versus unconditioned rats. D3V dorsal third ventricle. Scale bar = 100  $\mu$ m. Magnification is same in ‘a–f’

### Effect of conditioning on the expression of NMDA receptor subunit NR1 in the AcbSh

A significant increase in the frequency of puncta representing NR1 subunit was noticed ( $p < 0.001$ ) in the AcbSh of the ICSS-conditioned rats as compared to that in the unconditioned control rats (Fig. 5a–f).

### Effect of conditioning on the expression of CART mRNA in the LH

We examined the effect of ICSS conditioning on the expression of CART mRNA level in the LH–MFB. The ICSS-conditioned rats showed a significant increase in the CART mRNA expression ( $p < 0.001$ ) on the ipsilateral LH–MFB versus that in the contralateral side. However, there was no difference in the expression of CART mRNA across the tissues collected from the contralateral side of the conditioned and those from unconditioned rats (Fig. 6).

### DiI neuronal tracing study

The DiI injection in the AcbSh showed retrogradely labeled neurons in the PVT. Some of these neurons were colabeled with the CART antibody (Supplementary Fig. 4).

## Discussion

The LH–MFB area is an important site known to support ICSS (Wise 1996; Fulton et al. 2000). In the present study, the rats conditioned to self-stimulate via an electrode in the LH–MFB area showed an incremental lever press activity with the application of higher frequency. These results confirm our earlier findings (Desai et al. 2013; Somalwar et al. 2017) and are quite similar to those already reported in literature (Tomasiewicz et al. 2008).

### CART injected in PVT promotes ICSS behavior

Intra-PVT administration of CART, at the doses of 25 and 50 ng/rat, significantly facilitated the electrical self-stimulation; however, the lower dose (10 ng/rat) was ineffective. On the other hand, CART antibody injected into the PVT (to immunoneutralize endogenous CART locally) depressed the lever press activity, suggesting reward attenuation. These data are consistent with the range of studies attributing reward-promoting activity of the peptide (Kimmel et al. 2000; Philpot and Smith 2006; Upadhy et al. 2012; Somalwar et al. 2017). However, the role of CART in attenuating the reward and locomotor activity produced by the drugs of abuse has been underscored in

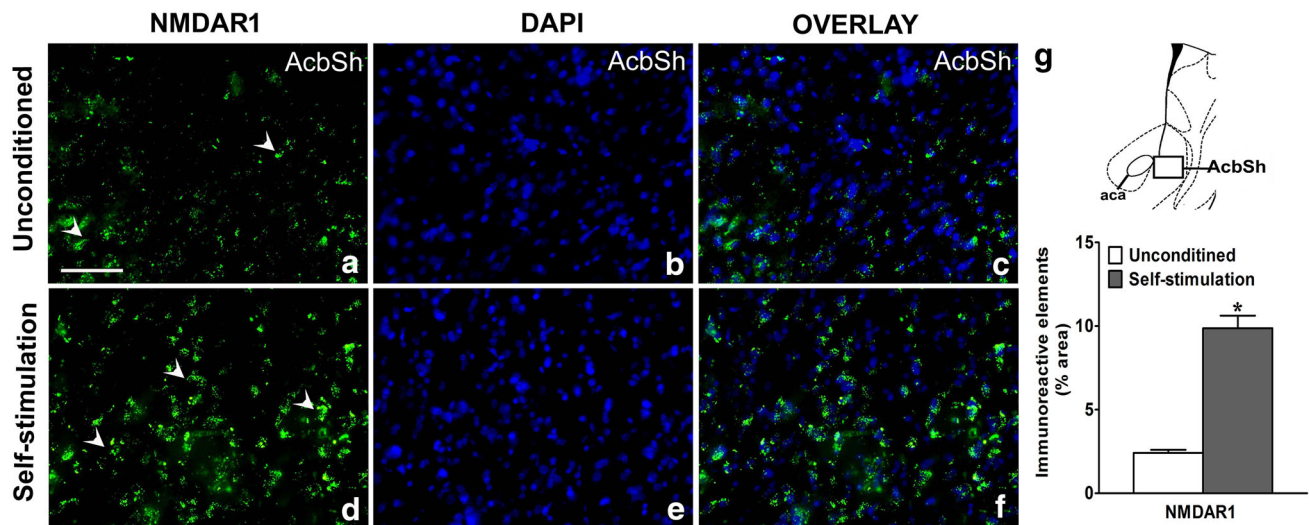


**Fig. 5** Coronal sections through the nucleus accumbens shell (AcbSh) showing the immunoreactive NMDAR1 elements (green; arrowheads; **a**, **d**), DAPI (blue; **b**, **e**) and overlay (NMDAR1 and DAPI; **c**, **f**) in unconditioned (**a–c**) and conditioned (**d–f**) rats. Data on the percent (%) immunoreactive area covered by NMDAR1-positive elements is represented in ‘g’ ( $n = 5$  in each group). The data were

collected from the demarcated rectangular area shown in the schematic (not to scale) taken from Paxinos and Watson (1998) coordinates (AP +0.7 mm to bregma). The data were analyzed by unpaired  $t$  test.  $*p < 0.001$  versus unconditioned rats. *aca* anterior commissure (anterior part). Scale bar = 100  $\mu$ m. Magnification is same in ‘a–f’

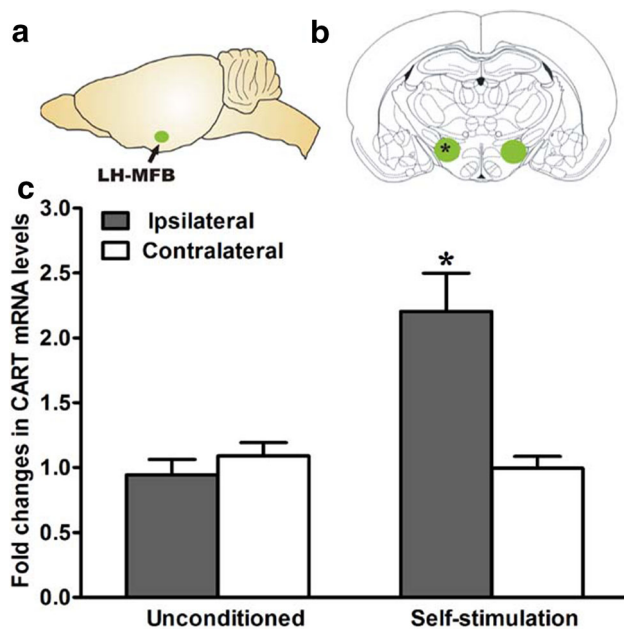


**Fig. 6** The effect of intracranial self-stimulation (ICSS) on CART mRNA expression in the lateral hypothalamus (LH)–medial forebrain bundle (MFB) area. The demarcated areas in ‘a’ and ‘b’ indicate the scope of tissue collected from the LH–MFB region (–1.8 to –2.8 mm with reference to bregma; Paxinos and Watson 1998). Asterisk in ‘b’ indicates the position of the electrode for ICSS. The data were analyzed by unpaired  $t$  test.  $*p < 0.001$  versus contralateral side or unconditioned rats

several studies (Jaworski et al. 2003; Yeoh et al. 2014; Kuhar 2016). It seems that the action of CART depends on the context to which the animal is exposed. This notion is

in agreement with the recent literature; Job and Kuhar (2017) have proposed that intra-Acb CART can promote or block rewarding behavior depending on the context (or type) of the reward. Furthermore, with specific reference to Acb, the direction of the effect of CART peptide is dependent on the level of activity of a psychostimulant, or on the baseline rate of the observed behavior (Job and Kuhar 2017).

#### CARTergic circuit from LH area to PVT may be up-regulated in the conditioned animals

The ICSS via an electrode implanted in the LH–MFB area induced an increase in the population of CART cells in the adjoining area with concomitant increase in c-Fos expression (Somalwar et al. 2017). The present study confirms these findings (data not shown). In addition, we report a more than twofold increase in CART mRNA expression in the ipsilateral LH–MFB versus the contralateral of the conditioned rats, as well that in the comparable tissue in unconditioned rats. This suggests activation of the CART gene, followed by transcription and translation of the CART peptide, as a function of electrical self-stimulation in the LH–MFB region. Concomitantly, the conditioned rats showed a robust increase in CART fibers in the PVT region bilaterally. The PVT of rat is known to receive CARTergic inputs from the LH–MFB area as well as arcuate nucleus (ARC), zona incerta and periventricular region of the hypothalamus (Kirouac et al. 2006). Therefore, the possibility of CARTergic innervations from these

sources cannot be ruled out. In sum, we suggest that the increase in the CART fiber density in the PVT, at least partly, may be due to the electrical stimulation of the CART neurons in the LH–MFB area.

### **ICSS behavior induces neuroadaptive changes in the PVT: involvement of CARTergic inputs**

In addition to the conspicuous increase in the population of CART fibers in the PVT of conditioned rats, the region showed a several-fold rise in the c-Fos expressing neurons in the conditioned rats versus that in unconditioned rats. The role of PVT in processing drug reward is well known. Acute administration of amphetamine and cocaine dose-dependently activated c-Fos expression in the PVT (Deutch et al. 1998; James et al. 2012; Matzeu et al. 2015). Since CART neurons in the LH–MFB area are known to project into the PVT (Parsons et al. 2006), we suggest that ICSS behavior might up-regulate the PVT neurons, and CARTergic inputs from LH may play an important role in the process. In the light of the information that CART neurons of the LH innervate the PVT (Kirouac et al. 2006; James et al. 2012), we suggest that in the conditioned animals, there might be an increase in the CARTergic innervation from the LH to PVT.

In view of the rich occurrence of glutamatergic neurons in the PVT (Frassoni et al. 1997; Parsons et al. 2007), we suggest that at least some of the c-Fos expression seen in the conditioned rats represents activation of the glutamatergic neurons. The PVT is a major source of glutamate neurons (Frassoni et al. 1997), and *in situ* hybridization studies have shown that glutamatergic cells in the PVT express vGLUT2 (Herzog et al. 2001; Huang et al. 2006). We found that CART and vGLUT2 immunoreactive elements increased dramatically with extensive overlappings in the frame of PVT in the conditioned animals. Therefore, the possibility exists that the conditioning experience may strengthen communication between CART afferents and the recipient glutamatergic neurons of the PVT. However, electron microscopy studies will be essential to reveal the synaptic contact between the neurons. In recent years, the role of PVT in modulating mesolimbic reward circuitry has been emphasized (Parsons et al. 2007; Matzeu et al. 2014). Neuronal tracing studies have shown that PVT receives strong neuronal afferents from the LH (Van der Werf et al. 2002; Thompson and Swanson 2003) and the information is transmitted onward to the Acb and mPFC using glutamate (Otake et al. 1995; Cornwall and Phillipson 1988; Li and Kirouac 2012; Kirouac et al. 2006). Electrophysiological studies have shown that hypocretin/orexins neurons in the LH project into the PVT and activate the vGLUT2-positive neurons (Huang et al. 2006). In this background, we suggest that ICSS via the LH–MFB might activate the

CARTergic inputs to the PVT, which in turn may promote glutamatergic PVT signaling to modulate the reward behavior.

### **Glutamate in the PVT–AcbSh circuit may mediate the rewarding action of CART**

The role of glutamatergic system in reward processing in the PVT–AcbSh circuit is well established. The PVT is a major source of glutamate neurons (Frassoni et al. 1997) and their glutamatergic fiber projections were detected in close vicinity to the tyrosine hydroxylase (TH)-positive (dopaminergic) axons in the AcbSh (Pinto et al. 2003). Blockade of glutamate receptors attenuated the PVT-evoked glutamate release in the AcbSh following electrical stimulation (Parsons et al. 2007). Intra-Acb infusion of NMDA receptor antagonist attenuated the facilitating effect of brain stimulation reward (Bespalov Aiu and Evartau 1996). Blockade of NMDA receptors attenuated morphine-induced CPP and reduced the extinction period of morphine reward (Ma et al. 2006; Siahposht-Khachaki et al. 2016). Systemic administration of MK-801 showed extinction deficit in appetitive operant tasks (Holahan et al. 2012). In the present study, intra-AcbSh administration of MK-801 (NMDA antagonist) decreased the lever press activity and elevated the ICSS threshold in a dose-dependent manner, suggesting the involvement of glutamatergic receptors. However, it is possible that the micro-infusions targeted at the AcbSh might diffuse into adjoining areas such as ventral palladium and the bed nucleus of stria terminalis. With a view to evaluate the involvement of glutamatergic system in the rewarding effects of CART, the combination study was undertaken. At the sub-effective dose, MK-801 prevented the rewarding activity of CART given directly in the PVT. DA released from the VTA is regulated by CART either directly or through disinhibition of GABAergic interneurons (Jaworski and Jones 2006). Several studies suggest that CART may act through inhibitory  $G_{i/o}$ -G-protein coupled receptor (GPCR) (Yermolaieva et al. 2001; Lakatos et al. 2005; Lin et al. 2011). However, in the current study, CART administered in the PVT is found to promote reward. The discrepancy may be explained as follows. There is a possibility that CART might exert its effects via some, as yet undetermined, type of disinhibition. Elias et al. (2001) have demonstrated that 67% CART cells in the LH contain GABA. We speculate that at least some of these neurons might communicate with the glutamatergic neurons of the PVT and exert their effect by disinhibiting the PVT neurons, which in turn may positively modulate DA release in the AcbSh to induce reward activity.

The NMDA receptor is a subtype of ionotropic glutamate receptors and regulates the synaptic plasticity in

excitatory synapses of the reward pathway (Sikora et al. 2016). The NMDA receptors expressed in the mesolimbic reward pathway have been implicated in processing synaptic plasticity, locomotor sensitization, reward-related learning and drug addiction (Smith-Roe and Kelley 2000; Ma et al. 2006; Siahposht-Khachaki et al. 2016; Sikora et al. 2016; den Hartog et al. 2017). Concurrent activation of DA and NMDA receptors in the Acb core is a prerequisite for acquisition of appetitive instrumental learning (lever press activity) (Smith-Roe and Kelley 2000). An exposure to natural reward (sexual experience) transiently increased NMDA receptor (NMDAR1 subunit) expression in the AcbSh (Pitchers et al. 2012) and acute/repeated administration of drugs of abuse such as cocaine or ethanol altered the NMDA receptor expression in the Acb (Wolf 2010; den Hartog et al. 2017) and VTA (Fitzgerald et al. 1996). Selective inactivation of NMDA receptors (NR1 subunit) on DA neurons significantly impaired the long-term potentiation in the Acb and also attenuated the drug (cocaine, morphine or ethanol)-induced CPP (Sikora et al. 2016). These data strongly implicate NMDA receptors in neuroadaptive changes following exposure to natural reward or drugs of abuse. Therefore, we sought to examine the effect of ICSS conditioning on NMDA receptors subtype NR1 expression in the reward pathway. We found that electrical stimulation in the LH–MFB area significantly enhanced the expression of NR1 subunit in the AcbSh.

### Role of the LH–PVT–AcbSh circuit in mediating reward

The LH–MFB area is a rich assemblage of neurons containing orexin, NPY, MCH, neurotensin and CART, and the involvement of these neuropeptides in arousal, feeding

and reward has been suggested (Bharne et al. 2015; James et al. 2017; Walker and Lawrence 2017). Orexin neurons from the LH colocalize with glutamate, the two agents are co-released and evoke glutamatergic release in the PVT (Schöne et al. 2012; Kolaj et al. 2014). Involvement of hypothalamic orexin neurons in mediating ethanol or cocaine reward-seeking behavior in the PVT is well established (Dayas et al. 2008; James et al. 2011). The role of orexin neurons in processing arousal, energy balance and reward-related information over the LH–PVT–Acb pathway has been suggested (Kelley et al. 2005; Matzeu et al. 2015, 2016). The orexins and CART are co-expressed within presynaptic sites and these peptides may be released in the synaptic cleft to modulate the postsynaptic neuron (Smith et al. 1999; Parsons et al. 2006). CART or orexin is found to colocalize with synaptophysin on fiber enlargements in the PVT (Kirouac et al. 2005, 2006). Interestingly, orexin as well as CART fibers were seen close to the PVT neurons, which were retrogradely labeled from the AcbSh (Parsons et al. 2006). On similar lines, hypothalamic CART/NPY neurons make synaptic contact with PVT soma that sends divergent axon collaterals to AcbSh (Lee et al. 2015). Almost all CART neurons in the LH colocalize with MCH, a neuropeptide involved in the regulation of feeding behavior (Vrang et al. 1999). Electrophysiological studies have demonstrated that hypothalamic hypocretins/orexin neurons strongly excite the glutamatergic neurons of the PVT (Huang et al. 2006). These investigations indicate that apart from CART, other agents in the LH system may be involved in modulating the PVT neurons. It would be interesting to probe the role of orexin, MCH and NPY in the LH in mediating brain stimulation reward.

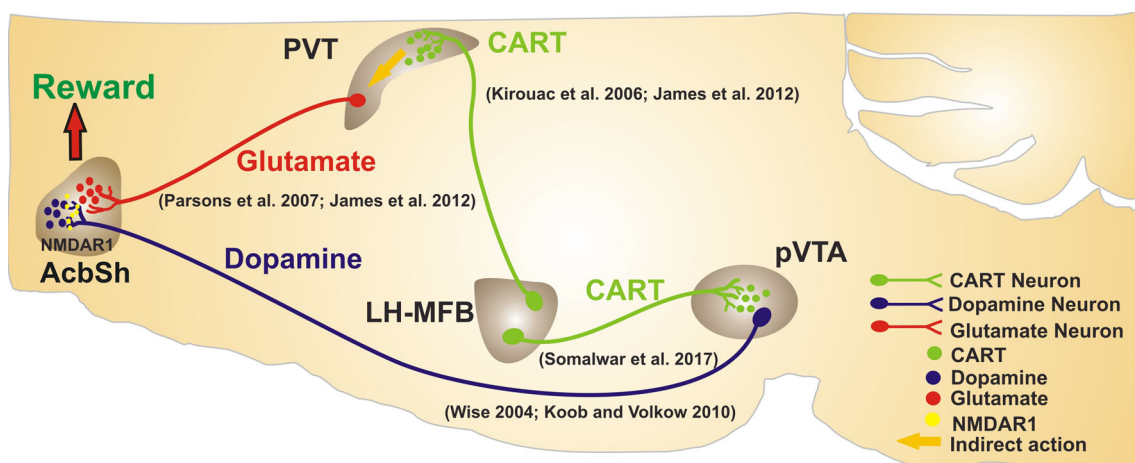


**Fig. 7** Hypothesized mechanism: The pVTA neurons communicate with the nucleus accumbens shell AcbSh over the dopaminergic mesolimbic pathway. CART neurons in the lateral hypothalamus (LH)–medial forebrain bundle (MFB) area communicate with the

posterior ventral tegmental area (pVTA) and paraventricular nucleus of thalamus (PVT). The information from the PVT may be conveyed to the (AcbSh) over the glutamatergic fibers, which in turn may modulate the reward behavior via NMDAR1 receptors

## Role of CART in modulating reward behavior: hypothesized mechanism

The CARTergic neuronal population in the LH–MFB area seems to project into the PVT where the peptide via an indirect action may influence the glutamatergic neurons. The glutamatergic projection, in turn, may communicate with the Acb and process reward behavior. Our earlier findings (Somalwar et al. 2017) suggest that the CART neurons residing in the LH–MFB region may communicate with the DA neurons in the pVTA and modulate the activity of the mesolimbic dopaminergic pathway. Kelley et al. (2005) have suggested the role for the LH–PVT–AcbSh pathway in food reward. Studies from our laboratory showed that rats fed on high-fat sweet palatable diet with reinforcing properties developed binge eating and showed concomitant up-regulation of CART neurons in the ARC–LH–PVT–AcbSh reward circuit (Bharne et al. 2015). Based on these emerging evidences, we suggest that under natural conditions, the CART neurons in the LH–MFB region may serve as an important player in mediating food reward. The hypothesized mechanism is schematically represented in Fig. 7.

**Acknowledgements** This work was supported by grants from the Science and Engineering Research Board (SERB) (SB/SO/AS-12/2014), Govt. of India, New Delhi, India to DMK. AJS acknowledges the grants from the UGC, Govt. of India, New Delhi, India [F.4-5/151-FRP/2014 (BSR)] and the BCUD, Savitribai Phule Pune University, Pune. AJS and SS also acknowledge the funds received from the DRDP of the Department of Biotechnology, Savitribai Phule Pune University, Pune, India. Confocal imaging was undertaken at IISER Pune Microscopy Facility, Pune, India.

### Compliance with ethical standards

**Conflict of interest** The authors declare no conflict of interest.

## References

- Bespalov Alu, Evartau EE (1996) The effect of the NMDA-receptor antagonist (+/-)-CPP on the conditioned-reflex activation of an operant reaction in the brain electrical self-stimulation test in rats. *Zh Vyssh Nerv Deiat Im I P Pavlova* 46:117–121
- Bharne AP, Borkar CD, Subhedar NK, Kokare DM (2015) Differential expression of CART in feeding and reward circuits in binge eating rat model. *Behav Brain Res* 291:219–231
- Carlezon WA Jr, Chartoff EH (2007) Intracranial self-stimulation (ICSS) in rodents to study the neurobiology of motivation. *Nat Protoc* 2:2987–2995
- Choi DL, Davis JF, Magrisso IJ, Fitzgerald ME, Lipton JW, Benoit SC (2012) Orexin signaling in the paraventricular thalamic nucleus modulates mesolimbic dopamine and hedonic feeding in the rat. *Neuroscience* 210:243–248
- Cornwall J, Phillipson OT (1988) Afferent projections to the dorsal thalamus of the rat as shown by retrograde lectin transport. II. The midline nuclei. *Brain Res Bull* 21:147–161
- Coulombe D, Miliareisis E (1987) Fitting intracranial self-stimulation data with growth models. *Behav Neurosci* 101:209–214
- Dandekar MP, Singru PS, Kokare DM, Lechan RM, Thim L, Clausen JT, Subhedar NK (2008) Importance of cocaine- and amphetamine-regulated transcript peptide in the central nucleus of amygdala in anxiogenic responses induced by ethanol withdrawal. *Neuropsychopharmacology* 33:1127–1136
- Dandekar MP, Singru PS, Kokare DM, Subhedar NK (2009) Cocaine- and amphetamine-regulated transcript peptide plays a role in the manifestation of depression: social isolation and olfactory bulbectomy models reveal unifying principles. *Neuropsychopharmacology* 34:1288–1300
- Dayas CV, McGranahan TM, Martin-Fardon R, Weiss F (2008) Stimuli linked to ethanol availability activate hypothalamic CART and orexin neurons in a reinstatement model of relapse. *Biol Psychiatry* 63:152–157
- den Hartog CR, Gilstrap M, Eaton B, Lench DH, Mulholland PJ, Homanics GE, Woodward JJ (2017) Effects of repeated ethanol exposures on NMDA receptor expression and locomotor sensitization in mice expressing ethanol resistant NMDA receptors. *Front Neurosci* 11:84
- Desai SJ, Upadhyaya MA, Subhedar NK, Kokare DM (2013) NPY mediates reward activity of morphine, via NPY Y1 receptors, in the nucleus accumbens shell. *Behav Brain Res* 247:79–91
- Desai SJ, Bharne AP, Upadhyaya MA, Somalwar AR, Subhedar NK, Kokare DM (2014) A simple and economical method of electrode fabrication for brain self-stimulation in rats. *J Pharmacol Toxicol Methods* 69:141–149
- Deutch AY, Bubser M, Young CD (1998) Psychostimulant-induced Fos protein expression in the thalamic paraventricular nucleus. *J Neurosci* 18:10680–10687
- Elias CF, Lee CE, Kelly JF, Ahima RS, Kuhar M, Saper CB et al (2001) Characterization of CART neurons in the rat and human hypothalamus. *J Comp Neurol* 432:1–19
- Fitzgerald LW, Ortiz J, Hamedani AG, Nestler EJ (1996) Drugs of abuse and stress increase the expression of GluR1 and NMDAR1 glutamate receptor subunits in the rat ventral tegmental area: common adaptations among cross-sensitizing agents. *J Neurosci* 16:274–282
- Frasconi C, Spreafico R, Bentivoglio M (1997) Glutamate, aspartate and co-localization with calbindin in the medial thalamus. An immunohistochemical study in the rat. *Exp Brain Res* 115:95–104
- Fulton S, Woodside B, Shizgal P (2000) Modulation of brain reward circuitry by leptin. *Science* 287:125–128
- Hamlin AS, Clemens KJ, Choi EA, McNally GP (2009) Paraventricular thalamus mediates context-induced reinstatement (renewal) of extinguished reward seeking. *Eur J Neurosci* 29:802–812
- Herzog E, Belenchi GC, Gras C, Bernard V, Ravassard P, Bedet C, Gasnier B, Giros B, El Mestikawy S (2001) The existence of a second vesicular glutamate transporter specifies subpopulations of glutamatergic neurons. *J Neurosci* 21:181
- Holahan MR, Westby EP, Albert K (2012) Comparison of the MK-801-induced appetitive extinction deficit with pressing for reward and associated pERK1/2 staining in prefrontal cortex and nucleus accumbens. *Behav Brain Res* 228:194–202
- Huang H, Ghosh P, van den Pol AN (2006) Prefrontal cortex-projecting glutamatergic thalamic paraventricular nucleus-excited by hypocretin: a feedforward circuit that may enhance cognitive arousal. *J Neurophysiol* 95:1656–1668
- James MH, Dayas CV (2013) What about me...? The PVT: a role for the paraventricular thalamus (PVT) in drug-seeking behavior. *Front Behav Neurosci* 7:18
- James MH, Charnley JL, Jones E, Levi EM, Yeoh JW, Flynn JR, Smith DW, Dayas CV (2010) Cocaine- and amphetamine-regulated transcript (CART) signaling within the paraventricular

- thalamus modulates cocaine-seeking behaviour. *PLoS One* 5:e12980
- James MH, Charnley JL, Levi EM, Jones E, Yeoh JW, Smith DW, Dayas CV (2011) Orexin-1 receptor signalling within the ventral tegmental area, but not the paraventricular thalamus, is critical to regulating cue-induced reinstatement of cocaine-seeking. *Int J Neuropsychopharmacol* 14:684–690
- James MH, Yeoh JW, Graham BA, Dayas CV (2012) Insights for developing pharmacological treatments for psychostimulant relapse targeting hypothalamic peptide systems. *J Addict Res Ther S* 4:008
- James MH, Mahler SV, Moorman DE, Aston-Jones G (2017) A decade of orexin/hypocretin and addiction: where are we now? *Curr Top Behav Neurosci* 33:247–281
- Jaworski JN, Jones DC (2006) The role of CART in the reward/reinforcing properties of psychostimulants. *Peptides* 27:1993–2004
- Jaworski JN, Kozel MA, Philpot KB, Kuhar MJ (2003) Intracumbal injection of CART (cocaine-amphetamine regulated transcript) peptide reduces cocaine-induced locomotor activity. *J Pharmacol Exp Ther* 307:1038–1044
- Job MO, Kuhar MJ (2017) CART peptide in the nucleus accumbens regulates psychostimulants: correlations between psychostimulant and CART peptide effects. *Neuroscience* 348:135–142
- Jones MW, Kilpatrick IC, Phillipson OT (1989) Regulation of dopamine function in the nucleus accumbens of the rat by the thalamic paraventricular nucleus and adjacent midline nuclei. *Exp Brain Res* 76:572–580
- Kelley AE, Baldo BA, Pratt WE (2005) A proposed hypothalamic–thalamic–striatal axis for the integration of energy balance, arousal, and food reward. *J Comp Neurol* 493:72–85
- Kimmel HL, Gong W, Vechia SD, Hunter RG, Kuhar MJ (2000) Intra-ventral tegmental area injection of rat cocaine- and amphetamine-regulated transcript peptide 55–102 induces locomotor activity and promotes conditioned place preference. *J Pharmacol Exp Ther* 294:784–792
- Kirouac GJ (2015) Placing the paraventricular nucleus of the thalamus within the brain circuits that control behavior. *Neurosci Biobehav Rev* 56:315–329
- Kirouac GJ, Parsons MP, Li S (2005) Orexin (hypocretin) innervation of the paraventricular nucleus of the thalamus. *Brain Res* 1059:179–188
- Kirouac GJ, Parsons MP, Li S (2006) Innervation of the paraventricular nucleus of the thalamus from cocaine- and amphetamine-regulated transcript (CART) containing neurons of the hypothalamus. *J Comp Neurol* 497:155–165
- Kokare DM, Shelkar GP, Borkar CD, Nakhate KT, Subhedar NK (2011) A simple and inexpensive method to fabricate a cannula system for intracranial injections in rats and mice. *J Pharmacol Toxicol Methods* 64:246–250
- Kolaj M, Zhang L, Hermes ML, Renaud LP (2014) Intrinsic properties and neuropharmacology of midline paraventricular thalamic nucleus neurons. *Front Behav Neurosci* 8:132
- Koylu EO, Couceyro PR, Lambert PD, Ling NC, DeSouza EB, Kuhar MJ (1997) Immunohistochemical localization of novel CART peptides in rat hypothalamus, pituitary and adrenal gland. *J Neuroendocrinol* 9:823–833
- Kuhar MJ (2016) CART peptides and drugs of abuse: a review of recent progress. *J Drug Alcohol Res*. <https://doi.org/10.4303/jdar/235984>
- Kuhar MJ, Jaworski JN, Hubert GW, Philpot KB, Dominguez G (2005) Cocaine- and amphetamine-regulated transcript peptides play a role in drug abuse and are potential therapeutic targets. *AAPS J* 7:E259–E265
- Lakatos A, Prinster S, Vicentic A, Hall RA, Kuhar MJ (2005) Cocaine- and amphetamine-regulated transcript (CART) peptide activates the extracellular signal-regulated kinase (ERK) pathway in AtT20 cells via putative G-protein coupled receptors. *Neurosci Lett* 384:198–202
- Lee JS, Lee EY, Lee HS (2015) Hypothalamic, feeding/arousal-related peptidergic projections to the paraventricular thalamic nucleus in the rat. *Brain Res* 1598:97–113
- Li S, Kirouac GJ (2008) Projections from the paraventricular nucleus of the thalamus to the forebrain, with special emphasis on the extended amygdala. *J Comp Neurol* 506:263–287
- Li S, Kirouac GJ (2012) Sources of inputs to the anterior and posterior aspects of the paraventricular nucleus of the thalamus. *Brain Struct Funct* 217:257–273
- Li Y, Li S, Wei C, Wang H, Sui N, Kirouac GJ (2010a) Changes in emotional behavior produced by orexin microinjections in the paraventricular nucleus of the thalamus. *Pharmacol Biochem Behav* 95:121–128
- Li Y, Li S, Wei C, Wang H, Sui N, Kirouac GJ (2010b) Orexins in the paraventricular nucleus of the thalamus mediate anxiety-like responses in rats. *Psychopharmacology* 212:251–265
- Lin Y, Hall RA, Kuhar MJ (2011) CART peptide stimulation of G protein-mediated signaling in differentiated PC12 cells: identification of PACAP 6–38 as a CART receptor antagonist. *Neuropeptides* 45:351–358
- Livak KJ, Schmittgen TD (2001) Analysis of relative gene expression data using real-time quantitative PCR and the 2<sup>−</sup>ΔΔC<sub>T</sub> method. *Methods* 25:402–408
- Ma YY, Guo CY, Yu P, Lee DY, Han JS, Cui CL (2006) The role of NR2B containing NMDA receptor in place preference conditioned with morphine and natural reinforcers in rats. *Exp Neurol* 200:343–355
- Matzeu A, Zamora-Martinez ER, Martin-Fardon R (2014) The paraventricular nucleus of the thalamus is recruited by both natural rewards and drugs of abuse: recent evidence of a pivotal role for orexin/hypocretin signaling in this thalamic nucleus in drug-seeking behavior. *Front Behav Neurosci* 8:117
- Matzeu A, Weiss F, Martin-Fardon R (2015) Transient inactivation of the posterior paraventricular nucleus of the thalamus blocks cocaine-seeking behavior. *Neurosci Lett* 608:34–39
- Matzeu A, Kerr TM, Weiss F, Martin-Fardon R (2016) Orexin-A/hypocretin-1 mediates cocaine-seeking behavior in the posterior paraventricular nucleus of the thalamus via orexin/hypocretin receptor-2. *J Pharmacol Exp Ther* 359:273–279
- Moga MM, Weis RP, Moore RY (1995) Efferent projections of the paraventricular thalamic nucleus in the rat. *J Comp Neurol* 359:221–238
- Nakhate KT, Dandekar MP, Kokare DM, Subhedar NK (2009) Involvement of neuropeptide Y Y1 receptors in the acute, chronic and withdrawal effects of nicotine on feeding and body weight in rats. *Eur J Pharmacol* 609:78–87
- Negus SS, Miller LL (2014) Intracranial self-stimulation to evaluate abuse potential of drugs. *Pharmacol Rev* 66:869–917
- Neumann PA, Wang Y, Yan Y, Wang Y, Ishikawa M, Cui R, Huang YH, Sesack SR, Schlüter OM, Dong Y (2016) Cocaine-induced synaptic alterations in thalamus to nucleus accumbens projection. *Neuropsychopharmacology* 41:2399–2410
- Otake K, Ruggiero DA, Nakamura Y (1995) Adrenergic innervation of forebrain neurons that project to the paraventricular thalamic nucleus in the rat. *Brain Res* 697:17–26
- Parsons MP, Li S, Kirouac GJ (2006) The paraventricular nucleus of the thalamus as an interface between the orexin and CART peptides and the shell of the nucleus accumbens. *Synapse* 59:480–490
- Parsons MP, Li S, Kirouac GJ (2007) Functional and anatomical connection between the paraventricular nucleus of the thalamus and dopamine fibers of the nucleus accumbens. *J Comp Neurol* 500:1050–1063

- Paxinos G, Watson C (1998) The rat brain in stereotaxic coordinates, 4th edn. Academic Press, New York
- Philpot K, Smith Y (2006) CART peptide and the mesolimbic dopamine system. *Peptides* 27:1987–1992
- Pinto A, Jankowski M, Sesack SR (2003) Projections from the paraventricular nucleus of the thalamus to the rat prefrontal cortex and nucleus accumbens shell: ultrastructural characteristics and spatial relationships with dopamine afferents. *J Comp Neurol* 459:142–155
- Pitchers KK, Schmid S, Di Sebastiano AR, Wang X, Laviolette SR, Lehman MN, Coolen LM (2012) Natural reward experience alters AMPA and NMDA receptor distribution and function in the nucleus accumbens. *PLoS One* 7:e34700
- Rademacher DJ, Sullivan EM, Figge DA (2010) The effects of infusions of CART 55–102 into the basolateral amygdala on amphetamine-induced conditioned place preference in rats. *Psychopharmacology* 208:499–509
- Sakharkar AJ, Zhang H, Tang L, Baxstrom K, Shi G, Moonat S, Pandey SC (2014) Effects of histone deacetylase inhibitors on amygdaloid histone acetylation and neuropeptide Y expression: a role in anxiety-like and alcohol-drinking behaviours. *Int J Neuropsychopharmacol* 17:1207–1220
- Schöne C, Cao ZF, Apergis-Schoute J, Adamantidis A, Sakurai T, Burdakov D (2012) Optogenetic probing of fast glutamatergic transmission from hypocretin/orexin to histamine neurons in situ. *J Neurosci* 32:12437–12443
- Siahposht-Khachaki A, Fatahi Z, Haghparast A (2016) Reduction of the morphine maintenance by blockade of the NMDA receptors during extinction period in conditioned place preference paradigm of rats. *Basic Clin Neurosci* 7:341–350
- Sikora M, Tokarski K, Bobula B, Zajdel J, Jastrzębska K, Cieślak PE, Zygmunt M, Sowa J, Smutek M, Kamińska K, Gołombiowska K, Engblom D, Hess G, Przewlocki R, Rodriguez Parkitna J (2016) NMDA receptors on dopaminergic neurons are essential for drug-induced conditioned place preference. *eNeuro* 3(3). <https://doi.org/10.1523/ENEURO.0084-15.2016>
- Smith Y, Kieval J, Couceyro PR, Kuhar MJ (1999) CART peptide immunoreactive neurones in the nucleus accumbens in monkeys: ultrastructural analysis, colocalization studies, and synaptic interactions with dopaminergic afferents. *J Comp Neurol* 407:491–511
- Smith-Roe SL, Kelley AE (2000) Coincident activation of NMDA and dopamine D1 receptors within the nucleus accumbens core is required for appetitive instrumental learning. *J Neurosci* 20:7737–7742
- Somalwar AR, Shelkar GP, Subhedar NK, Kokare DM (2017) The role of neuropeptide CART in the lateral hypothalamic-ventral tegmental area (LH–VTA) circuit in motivation. *Behav Brain Res* 317:340–349
- Thompson RH, Swanson LW (2003) Structural characterization of a hypothalamic visceromotor pattern generator network. *Brain Res Brain Res Rev* 41:153–202
- Tomasiewicz HC, Todtenkopf MS, Chartoff EH, Cohen BM, Carlezon WA Jr (2008) The kappa-opioid agonist U69,593 blocks cocaine-induced enhancement of brain stimulation reward. *Biol Psychiatry* 64:982–988
- Upadhyaya MA, Nakhate KT, Kokare DM, Singh U, Singru PS, Subhedar NK (2012) CART peptide in the nucleus accumbens shell acts downstream to dopamine and mediates the reward and reinforcement actions of morphine. *Neuropharmacology* 62:1823–1833
- Van der Werf YD, Witter MP, Groenewegen HJ (2002) The intralaminar and midline nuclei of the thalamus. Anatomical and functional evidence for participation in processes of arousal and awareness. *Brain Res Brain Res Rev* 39:107–140
- Vertes RP, Hoover WB (2008) Projections of the paraventricular and paratenial nuclei of the dorsal midline thalamus in the rat. *J Comp Neurol* 508:212–237
- Vrang N, Larsen PJ, Clausen JT, Kristensen P (1999) Neurochemical characterization of hypothalamic cocaine-amphetamine-regulated transcript neurons. *J Neurosci* 19:RC5
- Walker LC, Lawrence AJ (2017) The role of orexins/hypocretins in alcohol use and abuse. *Curr Top Behav Neurosci* 33:221–246
- Wise RA (1996) Addictive drugs and brain stimulation reward. *Annu Rev Neurosci* 19:319–340
- Wolf ME (2010) Regulation of AMPA receptor trafficking in the nucleus accumbens by dopamine and cocaine. *Neurotox Res* 18:393–409
- Yang SC, Pan JT, Li HY (2004) CART peptide increases the mesolimbic dopaminergic neuronal activity: a microdialysis study. *Eur J Pharmacol* 494:179–182
- Yeoh JW, James MH, Graham BA, Dayas CV (2014) Electrophysiological characteristics of paraventricular thalamic (PVT) neurons in response to cocaine and cocaine- and amphetamine-regulated transcript (CART). *Front Behav Neurosci* 8:280
- Yermolaieva O, Chen J, Couceyro PR, Hoshi T (2001) Cocaine- and amphetamine-regulated transcript peptide modulation of voltage-gated Ca<sup>2+</sup> signaling in hippocampal neurons. *J Neurosci* 21:7474–7480
- Young CD, Deutch AY (1998) The effects of thalamic paraventricular nucleus lesions on cocaine-induced locomotor activity and sensitization. *Pharmacol Biochem Behav* 60:753–758